

Independent Control of Three Magnetic Microrobots in Three Dimensions

Ryan Zeyuan Chen*, Jack Chen*, and David Qiyi Liu*

I. INTRODUCTION

A microrobot is a small-scale robot with characteristic dimensions less than 1 mm. Due to their small size and high mobility, microrobots show great potential for biomedical applications such as disease diagnosis, health monitoring, targeted drug delivery and minimally invasive surgery [1]. While various actuation methods exist for microrobots, magnetic actuation has been identified as a suitable technique for realizing three-dimensional control in confined environments. Since an external magnetic actuation system can safely and remotely generate torques and forces on the micro-robot, it is ideal for *in situ* operations [1].

In addition to the utilization of a single robot for these tasks, the capability to deploy multiple microrobots will enable more precise application scenarios as well as significantly improve operation efficiency. While implementing control strategies for a single magnetic microrobot can be relatively straightforward, independently controlling multiple magnetic microrobots is shown to be quite challenging since the robots are subjected to global magnetic fields. In order to realize more complex microbotic applications, overcoming the challenge of multi-agent control has becomes a significant focal point of the microrobots research community in recent years [2].

In this work, we explore the independent and robust control of three microswimmers in three dimensions. Microscale applications require the independent control of multiple microrobots working together to manipulate microscale objects to achieve complex tasks. The proposed method could enable independent control of three microrobots *in vitro* inside microfluidic channels or *in vivo* inside humans, with potential applications for localized therapy and microscale manipulation. The main contributions of this project is the extension of a previous method for independent control of two microswimmers in two dimensions to three microswimmers in three dimensions [3]. Though the ideal simulation environment limits the applications of this work to real-world conditions, the investigation of the fundamental magnetic actuation methods serves as

This work was completed as a part of the course MIE505 Micro/Nano Robotics at the University of Toronto.

All authors are with the Division of Engineering Science, University of Toronto, Toronto, ON M5S 1A4, Canada. {zeyuan.chen, jackhao.chen, qiyi.liu}@mail.utoronto.ca

*These authors contributed equally.

an important first step for future work. More complex and robust methods can be developed by extending the experimental principles and characterizations in this report.

II. OBJECTIVES

The main objective of the project was to accurately and independently control three microswimmers in water. The objective is met if the steady-state error of the implemented control strategy is less than 10% under all conditions. To further evaluate the performance of various control strategies, each microswimmer is controlled to draw the letters "M", "I", and "E" in the x-y, y-z and x-z planes respectively in simulation with added real-world noise.

This goal was achieved in the following four steps:

- Create a workable basic 3D simulation environment which can simulate basic physics interactions between the microswimmers, water, and magnetic field.
- Independently control three microswimmers to draw the letters "M", "I", and "E" in their respective planes in the simulation environment with no noise. The location error for each robot should be less than 5 % .
- Improve the basic 3D simulation environment by adding modelled real-world noises.
- Independently control three microswimmers to draw complex designs in the noisy simulation environment, which resembles the real-world environment. The location error for each robot should be less than 10 % .

III. METHODS

A. Simulation Environment

Due to the constraints of the COVID-19 pandemic, we develop and demonstrate independent control of three microswimmers in a simulated environment with Python3 and the NumPy, Matplotlib, SciPy, and OpenCV libraries. A state-space model is derived using magnetic equations developed in class, and the model is then discretized to enable numerical simulation. The simulation environment models various forms of measurement noises to represent operation in real-world environments. We initially developed a no-noise environment to test their respective theoretical best performance, while the robustness of the controllers

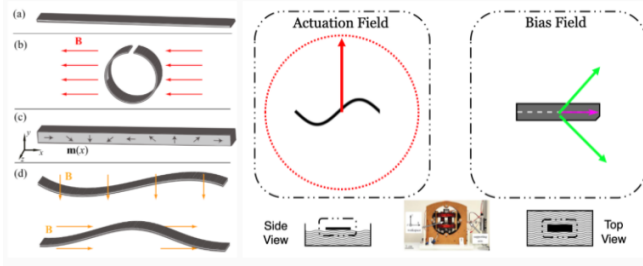


Fig. 1. Magnetization and Actuation Method of Magnetic Microswimmers, from MIE505 Lecture 8

will be tested in the close-to-real-world simulation environment. The best performed controller can be chosen based on the simulation result.

B. Magnetic Microswimmer

As derived in class, the magnetic force F and magnetic torque τ are as follows [4].

$$F = \mu_0 v (M * \nabla) H$$

$$\tau = \mu_0 v M \times H$$

The equations can be directly applied because the magnetization vector M is independent of the applied field. The magnetic fields are applied by multiple pairs of Helmholtz coils, which ensure an uniform total field inside the coil pairs.

In simulation, we will model the microswimmers used in the MIE505 labs [5]. We assume that the microswimmer is fabricated with modified proportions of EcoFlex and magnetic beads to give it a density that ensures neutral buoyancy. Fig. 1 shows the magnetization and actuation of the microswimmer. The sinusoidal magnetizaton pattern allows a rotating magnetic field in the perpendicular direction to create a travelling wave, actuating the robot. Magnetic fields in the other directions bias the microswimmer's direction. In tandem, the actuating and bias field allows the microswimmer to translate and rotate freely [6].

C. Extension to Three Microswimmers in 3D

To enable independent control of three microswimmers, we will align each robot with a separate actuation plane. Fig. 2 shows the global reference frame of the environment, with all robots perpendicular to each other. Consider the robot reference frame in Fig. 2 for Robot 1. A rotating actuation field in the y - z plane creates a travelling wave in Robot 1, but not in Robots 1 and 2. Thus, Robot 1 can be actuated independently.

All robots are under the influence of the same magnetic forces and torques in the experimental setup. They are inherently linked, and bias fields will rotate all robots at the same time. However, with the proposed setup, the robots will all rotate together, and their actuation planes will always remain perpendicular. Fig. 10 in the Appendix shows the three different orientations

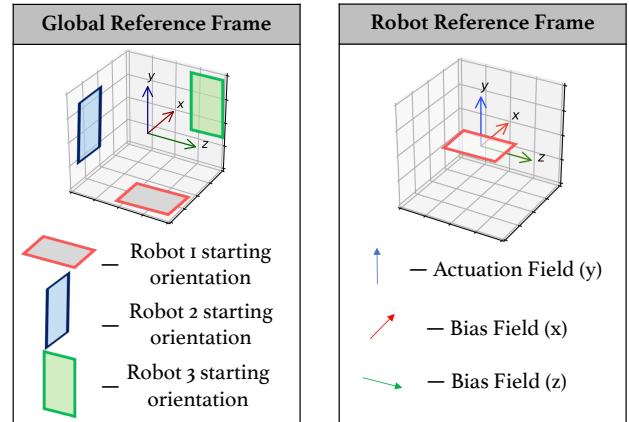


Fig. 2. Global and local references frame of the simulation environment

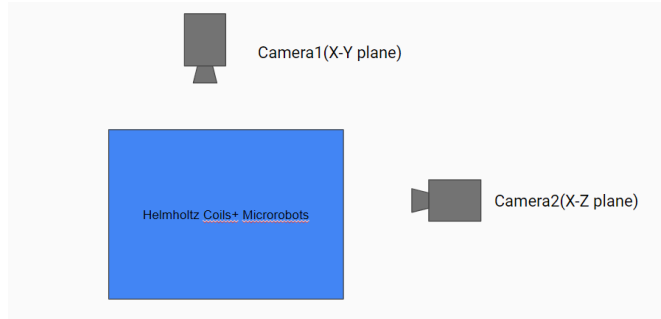


Fig. 3. Virtual visual servoing setup with two cameras.

of the the robots in the experiment. Each orientation can be biased to another orientation with a rotation of 90 degrees. In each orientation, each robot is actuated with a rotating actuation field in a perpendicular plane. Thus, the controller can be designed to move one robot at a time to the desired goal point. When one robot's motion is complete, the bias field can be applied to actuate the next robot.

D. Visual Servoing

In order to have a realistic measurement input for the control algorithm. A virtual cameras motion tracking setup is used to simulate the real-world motion tracking method as shown in Fig. 3. The physical location of the microrobots is represented in a 3 dimensional matrix. The 3 d matrix will be compressed along z axis and y -axis to get x - y and x - z plane information respectively. The compressed x - y and x - z plane matrices will be considered as the images taken by the Camera1 and Camera2. The measured position of microrobots is generated by applying Eigentracking algorithm. When 2 robots overlap each other in x - y plane, and they can be distinguished in x - z plane, the robots can still be tracked accurately in x - y plane using the information of the x - z plane. The measurement input for the close loop control system with PID control will the motion information extracted from the trackers on 2 cameras'

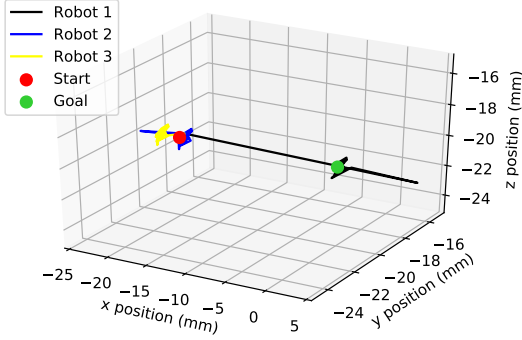


Fig. 4. PID Controller of Actuation Fields for Independent Position Control. While Robot 1 moves from initial to goal point, Robots 2 and 3 remain at the initial point.

images. This is a more realistic measurement than just put in the accurate position information as the measurement for the controller.

IV. RESULTS

A. Control

To control the robots orientation and position, we designed a PID controller for the actuation and bias fields [7]. The PID gains were tuned using the Ziegler-Nichols method. Due to the scaling laws at the microswimmers scale, small changes in the applied force and torque caused large system outputs. The integral and derivative gains tended to make the system unstable. After much experimentation, the optimal PID controller had a larger proportional gain with log integral and derivative gains.

Fig. 4 shows the PID controller providing independent actuation control on a robot with Gaussian measurement noise. The rotating actuation field produces a travelling wave in robot 1 only, allowing it to move from initial position in red to the goal position. Simultaneously, robots 2 and robot 3 remain at the initial position but do not remain stationary due to system noise.

Fig. 5, Fig. 6, and Fig. 7 show the step response of the PID controller for actuation with Gaussian, Uniform, and Laplacian noise at varying parameters. The noise parameters were increased until the PID controller could no longer result in a stable response.

Table 1 in the Appendix summarizes the dynamic response characteristics of the system controller. Overall, the controller performs reasonably based on the design parameters. The rise time and settling is not very fast, especially at larger noises. However, slowing down the dynamic response improved the stability of the system. At microscale, a faster response is harder to control due to the extremely fast speeds of the microswimmer. The steady-state errors are very low

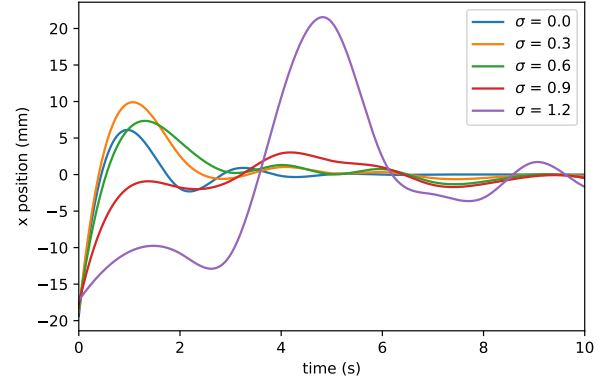


Fig. 5. Step Response of PID Controller with Gaussian Measurement Noise with Mean = 0 and Standard Deviation = σ

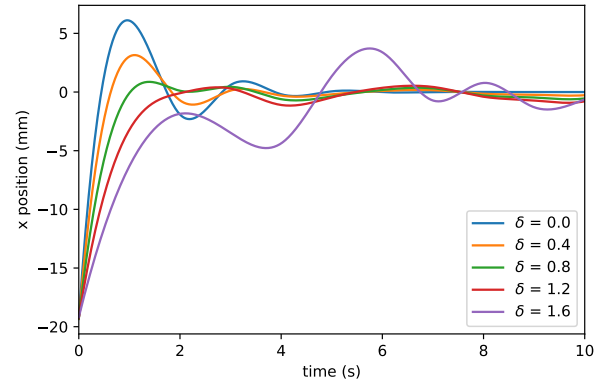


Fig. 6. Step Response of PID Controller with Uniform Measurement Noise with Mean = 0 and Interval = δ

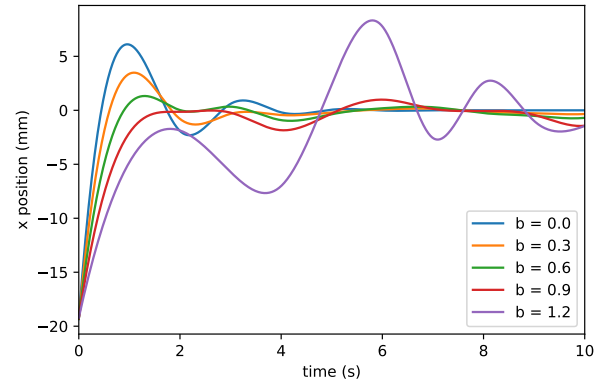


Fig. 7. Step Response of PID Controller with Laplacian Measurement Noise with Mean = 0 and Decay = b

for the simulated microswimmers. Eventually, the PID controller stabilizes the robot to the goal point, and the steady-state error simply becomes the measurement noise.

A separate PID controller was designed and tuned

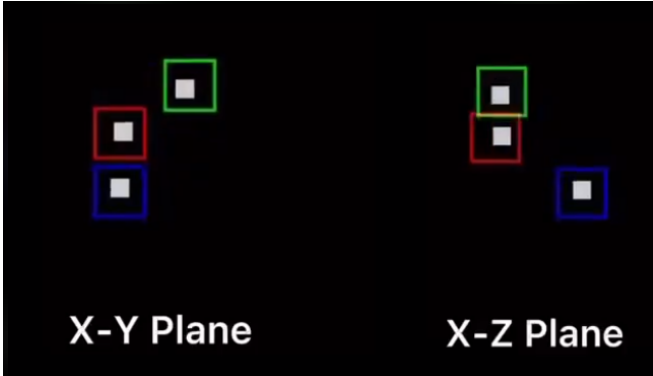


Fig. 8. An example visual tracking image produced using the visual servoing setup.

for the bias fields to orient the microswimmers. The dynamic characteristics were very similar, with the microswimmers exhibiting a slow response with low steady-state error.

B. Path Following

To evaluate the performance of the described modeling and control scheme, the three microrobots are independently controlled to follow various paths through waypoint following. The ideal trajectory for a given set of waypoints is the straight line connecting the previous goal point and the next goal point. The motion planning algorithm is set up such that a waypoint is considered to be reached once the microrobot comes within 0.5 mm of the goal. A Kalman filter is also applied utilizing the `pykalman` library to reduce system noise. The resulting path following performance of the control scheme is shown in Fig. 11 in the Appendix. The three robots are controlled to follow various designed paths independently, such as straight lines, squares, and the letters "MIE". It can be seen that the microrobots can follow the desired trajectories with relatively low errors despite the effects of disturbances caused by noise injected into the system.

C. Visual Servoing

An example visual tracking image using the visual servoing setup is presented in Fig. 8. The performance of the controller is able to maintain at a consistent level given measurement data produced from the setup. Therefore, the controller is relatively robust to resist the errors produced via the object tracking algorithm mimicking real-world scenarios.

V. DISCUSSION

A. Path Following

The cumulative distance travelled by each micro-robot following the straight line path in Fig. 11a is shown in Fig. 9. In the ideal case, since only a single microrobot is controlled to move at a given time, the

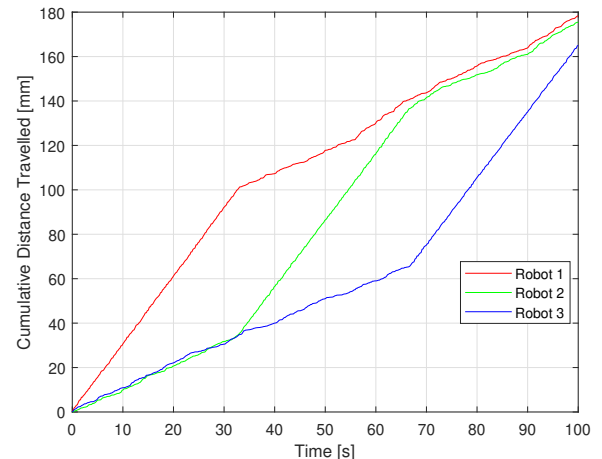


Fig. 9. The cumulative distance travelled by each microrobot following a straight line path.

cumulative distance travelled by the other two microrobots should remain at a constant value. However, since noise is injected into the simulation system, it can be seen that while one robot is in motion, the other two robots are also accumulating in distance at a lower rate. This is directly due to the fact that the other two robots will not remain stationary under the influence of system disturbances.

B. Limitations

In this project, all experimental data was obtained using simulated data. The major limitations of the results are due to the assumptions made in the simulation setup. In the MIE505 labs, we worked on the control of a single microswimmer in two dimensions. During the labs, the microswimmers were not perfectly fabricated with an exact sinusoidal magnetization. This means that the robot does not move in a perfect travelling wave. The robot would deviate from the desired path and become misaligned with the actuation plane. Deviations would be compounded by real-world friction, gravity, and fluid resistance [8]. Altogether, these factors pose a critical issue for our proposed methods. If the microswimmers' actuation fields due to remain perpendicular, multiple robots will actuate at simultaneously, making independent control extremely difficult.

Furthermore, the actual actuation and bias fields will not behave ideally as in simulation. During the MIE505 labs, the microswimmer would not align perfectly to the bias field, even after perfect calibration. Inconsistencies in the microswimmer fabrication, combined with the limitations of actual magnetic fields means that the microswimmers cannot be perfectly oriented in the desired direction. In addition, the Helmholtz coil system did not create a perfect uniform field in the MIE505 labs. Actuation of the robot near the

experiment boundaries resulted in noticeably different behavior than actuation in the center. The simulations of this project do not take these factors into account. Real-world control of three microswimmers with the proposed method would result in a much less stable system. The actuation of the three microswimmers would be coupled, resulting in worse performance.

A final limitation is that the work cannot be further extended to more microswimmers. Since all microswimmers must have perpendicular actuation planes, adding a fourth microswimmer would not be possible. Future work will involve applying the concepts learned in this project to develop a more advanced control method that can better resolve the inherent coupling between multiple magnetic robots. The method should be tested in a real-world environment setting rather than in simulations to resolve the discussed.

VI. CONCLUSION

The proposed independent control of three magnetic microrobots in three dimensions has reasonable performance under the simulation environment. It only has 5.5% path deviation error under the Gaussian noise with 12 mm standard deviation, which meets the requirement originally outlined by the project proposal.

In class, we learned about the independent control of two magnetic microswimmers and worked with these microswimmers in lab. This project is the natural extension of what we learned in class, applying the physical models we developed in three dimensions. Extending magnetic control to three dimensions brings magnetic microrobots closer to real-world applications. Robust independent control of three microswimmers would enable *in vitro* experiments in microfluidic channels and *in vivo* experiments in swine or humans. Interesting applications such as microscale cargo delivery, microscale manipulation, and localized therapy cannot be performed with one single microrobot, but rather requires the independent control of many microrobots. The concepts developed in this project form the first steps towards these realizing applications that require multiple, independent microrobots working together.

REFERENCES

- [1] M. Sitti, H. Ceylan, W. Hu, J. Giltinan, M. Turan, S. Yim, and E. Diller, “Biomedical applications of untethered mobile milli/microrobots,” *Proceedings of the IEEE*, vol. 103, no. 2, pp. 205–224, 2015.
- [2] S. Chowdhury, W. Jing, and D. J. Cappelleri, “Controlling multiple microrobots: recent progress and future challenges,” *Journal of Micro-Bio Robotics*, vol. 10, p. 1–11, 2015.
- [3] J. Zhang, P. Jain, and E. Diller, “Independent control of two millimeter-scale soft-bodied magnetic robotic swimmers,” in *2016 IEEE International Conference on Robotics and Automation (ICRA)*, 2016, pp. 1933–1938.
- [4] E. Diller, “*Magnetic Actuation 2: Field Creation and Use.*,” in *MIE505 Micro/Nano Robotics.*, 2021.
- [5] E. Diller, J. Zhuang, G. Zhan Lum, M. R. Edwards, and M. Sitti, “Continuously distributed magnetization profile for millimeter-scale elastomeric undulatory swimming,” *Applied Physics Letters*, vol. 104, no. 17, p. 174101, 2014.
- [6] M. Salehizadeh and E. Diller, “Three-dimensional independent control of multiple magnetic microrobots via inter-agent forces,” *The International Journal of Robotics Research*, vol. 39, no. 12, pp. 1377–1396, 2020.
- [7] S. T. Jingyi Wang, Niandong Jiao and L. Liu, “Automatic path tracking and target manipulation of a magnetic microrobot,” 2021.
- [8] M. Boudaoud, Y. Haddab, Y. Le Gorrec, and P. Lutz, “Noise characterization in millimeter sized micromanipulation systems.” *Mechatronics*, vol. 21, no. 6, pp. 1087–1097, Sep. 2011.

APPENDIX

TABLE I
STEP RESPONSE CHARACTERISTICS OF PID CONTROLLER WITH VARYING MEASUREMENT NOISE

Noise Type	Noise Parameter	Rise Time (s)	Overshoot (%)	Settling Time (s)	Steady-Steady Error (mm)
None	-	0.8	31.6	2.6	0.0
Gaussian	$\sigma = 0.3$	0.9	52.7	4.2	0.3
Gaussian	$\sigma = 0.6$	1.1	40.2	24.4	0.6
Gaussian	$\sigma = 0.9$	3.4	17.1	28.2	0.9
Gaussian	$\sigma = 1.2$	3.9	125	29.0	1.2
Uniform	$\delta = 0.4$	0.9	16.3	2.4	0.2
Uniform	$\delta = 0.8$	9.3	4.7	0.9	0.5
Uniform	$\delta = 1.2$	9.5	6.9	21.9	0.7
Uniform	$\delta = 1.6$	4.6	19.4	26.7	0.9
Laplacian	$b = 0.3$	0.9	18.1	21.1	0.3
Laplacian	$b = 0.6$	9.5	9.9	21.9	0.5
Laplacian	$b = 0.9$	9.6	16.1	26.4	0.8
Laplacian	$b = 1.2$	4.6	43.3	29.0	1.1

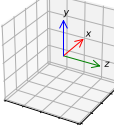
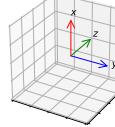
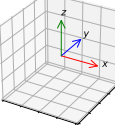
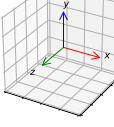
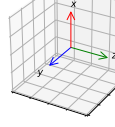
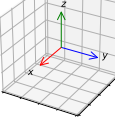
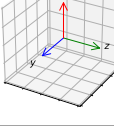
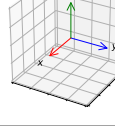
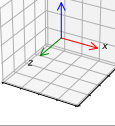
	Robot 1 Frame	Robot 2 Frame	Robot 3 Frame	Actuation Field (Global Frame)		
				xy plane	xz plane	yz plane
Orientation 1				Only robot 3 moves	Only robot 1 moves	Only robot 2 moves
Orientation 2				Only robot 2 moves (in the negative direction)	Only robot 1 moves	Only robot 3 moves
Orientation 3				Only robot 1 moves (in the negative direction)	Only robot 3 moves	Only robot 2 moves

Fig. 10. Three orientations for the microswimmers. In each orientation, microswimmers can be moved independently using rotating magnetic fields in different actuation planes.

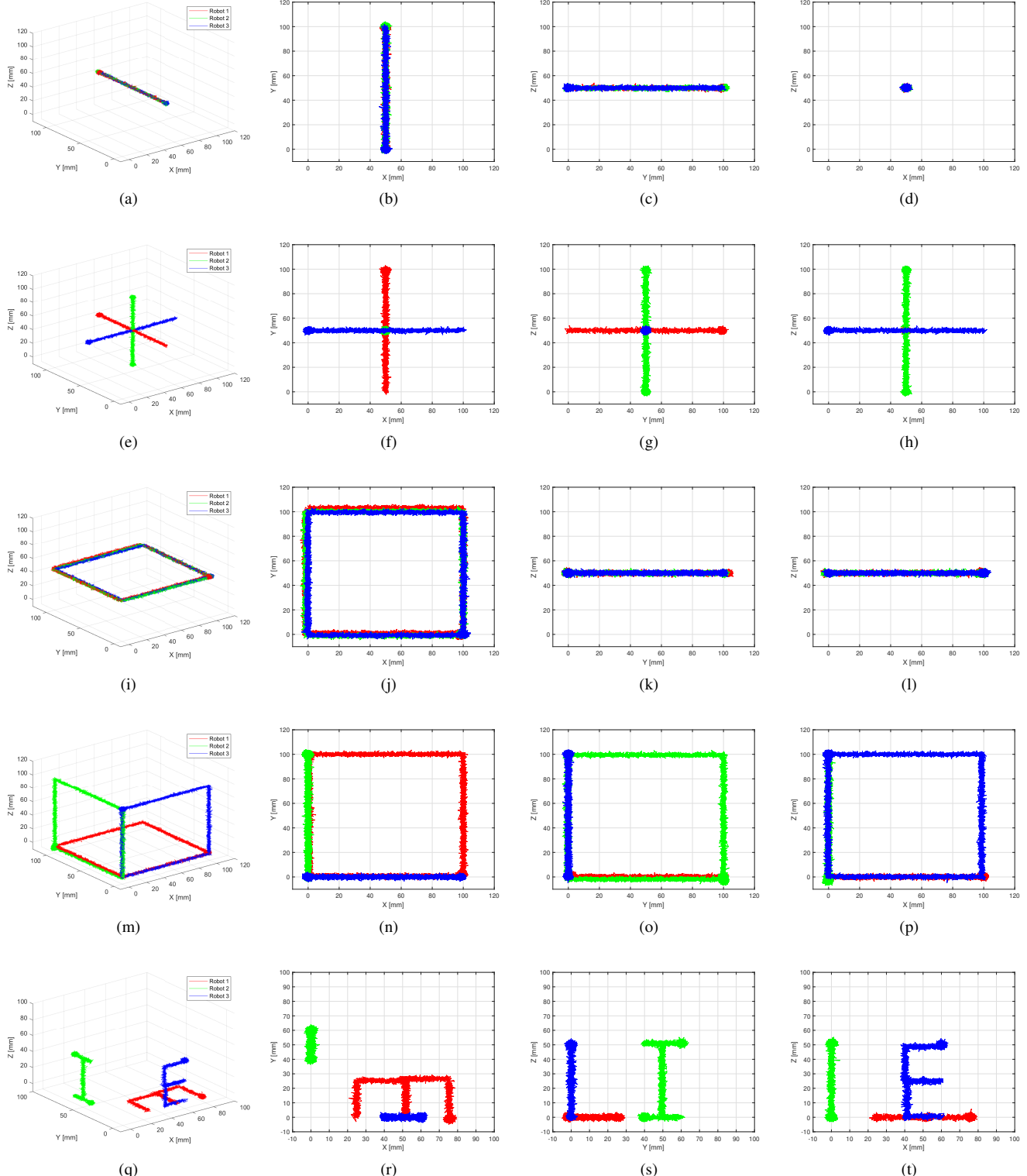


Fig. 11. Three microswimmers are controlled to follow various designed paths. (a), (e), (i), (m), (q) are the plotted microswimmer positions in 3D. (b), (f), (j), (n), (r) are the plotted microswimmer positions in the x-y plane. (c), (g), (k), (o), (s) are the plotted microswimmer positions in the y-z plane. (d), (h), (l), (p), (t) are the plotted microswimmer positions in the x-z plane. (a), (e) demonstrate the capabilities of the control scheme to facilitate the three microswimmers to follow straight line paths. (i), (m) demonstrate the microswimmer's ability to follow square paths with the implemented control strategy. (q) showcases the three microrobots moving in paths that draw out the letters "M", "I", and "E" in their respective planes.